

## Polaron Crossover and Bipolaronic Metal-Insulator Transition in the Half-Filled Holstein Model

M. Capone

*Enrico Fermi Center, Roma, Italy*

S. Ciuchi

*Istituto Nazionale di Fisica della Materia and Dipartimento di Fisica, Università dell'Aquila,  
via Vetoio, I-67010 Coppito-L'Aquila, Italy*

(Received 29 April 2003; published 30 October 2003)

The formation of a finite-density polaronic state is analyzed in the context of the Holstein model using the dynamical mean-field theory. The spinless and spinful fermion cases are compared to disentangle the polaron crossover from the bipolaron formation. The exact solution of dynamical mean-field theory is compared with weak-coupling perturbation theory, noncrossing (Migdal), and vertex correction approximations. We show that polaron formation is not associated with a metal-insulator transition, which is instead due to bipolaron formation.

DOI: 10.1103/PhysRevLett.91.186405

PACS numbers: 71.38.Ht, 71.10.Fd, 71.30.+h

Recent experiments strongly suggest that the electron-phonon (e-ph) interaction is relevant in many materials, ranging from high  $T_c$  superconducting cuprates [1], to colossal magnetoresistance manganites [2], from the fullerenes [3] to magnesium diboride [4]. While the specific role of the e-ph interaction is certainly very different from compound to compound, the properties of these materials are hardly explained in terms of standard approaches to the e-ph problem, like the Migdal-Eliashberg theory, and pose a serious challenge to theories.

More specifically, polaronic features have been observed in lightly doped cuprates [5], in the manganites [2], up to some indication in the fullerenes [6]. A small polaron is a carrier so tightly interacting with the lattice that its effective mass is strongly enhanced therefore reducing its mobility [7]. The single polaron problem has been extensively studied allowing one to understand in detail the polaron physics [8,9]. Nevertheless, the experimental findings of polaronic effects obviously deal with finite densities of carriers, and prompt for an analogous understanding of the finite-density polaron problem, where the polarons are able to interact and to change drastically the phonon properties. In this regard, it is important to stress the distinction between polaronic and bipolaronic states. If repulsion between the electrons is neglected, two polarons (with opposite spin) tend in fact to bind, giving rise to a (local) pair, which is called bipolaron. The bipolarons in turn may undergo a superconducting transition of the Bose-Einstein type [10]. If superconductivity is not allowed, bipolarons give rise to an insulating state of localized pairs [11,12] which may eventually condense in a charge-ordered state [13]. In some important compounds bipolaronic states are indeed unlikely formed. In cuprates and fullerenes, the strong electron correlation forbids bipolaron formation, while in the manganites, the double-exchange mechanism favors

ferromagnetic states at low temperature, in which no bipolaron can be formed.

In order to disentangle the polaron effects from bipolaron formation, we compare the spinless fermion case, in which bipolarons are forbidden by the Pauli principle, with the spinful case, which has been extensively studied in the recent past [14–18]. To be more explicit, we show that the polaron crossover at finite density is not by itself a metal-insulator transition (MIT), and insulating behavior can be associated only with localized bipolarons. This effect shows up in the nonvanishing of both the quasiparticle renormalization factor and the renormalized phonon frequency in the spinless case. In the spinful case the quasiparticle weight vanishes at some definite coupling while the renormalized phonon frequency remains finite.

We consider the Holstein molecular crystal model, in which tight-binding electrons interact with local modes of constant frequency. The Hamiltonian is

$$H = -t \sum_{\langle i,j \rangle, \sigma} c_{i,\sigma}^\dagger c_{j,\sigma} + \text{H.c.} - g \sum_i n_i (a_i + a_i^\dagger) + \omega_0 \sum_i a_i^\dagger a_i, \quad (1)$$

where  $c_{i,\sigma}$  ( $c_{i,\sigma}^\dagger$ ) and  $a_i$  ( $a_i^\dagger$ ) are destruction (creation) operators for fermions and for phonons of frequency  $\omega_0$ ,  $n_i$  is the electron density,  $t$  the hopping amplitude, and  $g$  is an e-ph coupling. The density is fixed to  $n = 0.5$  ( $n = 1$ ) in the spinless (spinful) system, which corresponds to the particle-hole symmetric half-filled case. In analogy with the studies of the Mott transition in the Hubbard model, in which antiferromagnetism is neglected [19], we restrict ourselves to the state with no charge order [12]. Despite the fact that in the particle-hole symmetric case the ground state is always ordered, the homogeneous solution may become representative of the

ground state whenever charge ordering is spoiled by some frustration effect such as a next-nearest-neighbor hopping. Moreover, this study allows one to characterize how strong e-ph interaction may lead to the destruction of the metallic state (just like electron correlation leads to the Mott state). The adiabatic ratio  $\gamma = \omega_0/t$  has been shown to be an important parameter for the single polaron formation. In the adiabatic regime  $\gamma < 1$ , the polaron crossover occurs when  $\lambda = g^2/\omega_0 t \simeq 1$ , while in the antiadiabatic regime  $\gamma > 1$ , the condition is instead  $(g/\omega_0)^2 \simeq 1$  [8,9].

We solve the model using the dynamical mean-field theory (DMFT), a nonperturbative approach which becomes exact in the limit of infinite dimensions [19]. We notice that in such a limit the spinless fermion case does not coincide with the infinite correlation limit. Nonetheless, this system represents an instructive playground where polaronic effects can be observed without too many competing phases. In DMFT, the lattice model is mapped onto an impurity problem subject to a self-consistency condition, which contains the information about the lattice. In our case the impurity model is

$$H = -\sum_{k,\sigma} V_k c_{k,\sigma}^\dagger f_\sigma + \text{H.c.} + \sum_{k,\sigma} E_k c_{k,\sigma}^\dagger c_{k,\sigma} - g(a + a^\dagger) \sum_{\sigma} f_\sigma^\dagger f_\sigma + \omega_0 a^\dagger a, \quad (2)$$

where the phonons live only on the impurity ( $f$ ) site,  $E_k$  and  $V_k$  are the energy levels and the hybridization parameters of the conduction bath. For the  $z$  coordination Bethe lattice of half bandwidth  $D = 2t\sqrt{z} = 1$  the self-consistency equation in the  $z \rightarrow \infty$  limit is

$$\frac{D^2}{4} G(i\omega_n) = \sum_k \frac{V_k^2}{i\omega_n - E_k}. \quad (3)$$

In this work we use exact diagonalization (ED) to solve the impurity model (2) [20]. This method requires one to restrict the sum in Eqs. (2) and (3) to a finite small number of levels  $N_s - 1$ . The discretized model can then be solved at  $T = 0$  using the Lanczos method. The convergence is exponential in  $N_s$ , and a few levels are enough to give converged results. Results are obtained taking typically  $N_s = 10$ , having checked that no significant change occurs for larger  $N_s$  [21]. Error bars can be evaluated by linearly extrapolating (in  $1/N_s$ ) to  $N_s \rightarrow \infty$  and are of the size of symbols in the figures. We compare the ED solution of DMFT, with two approximate schemes: a self-consistent noncrossing approximation (NCA) [11,15] [Fig. 1(a)] and a self-consistent approximation including the first vertex correction beyond NCA (VCA) [15] Figs. 1(a) and 1(b). Notice that in the standard Migdal-Eliashberg approximation the phonon spectrum is not self-consistently evaluated, but it is taken ‘‘from experiments,’’ while in our NCA and VCA the phonon self-energy is self-consistently evaluated (on the imaginary frequency axis) through an iterative scheme,

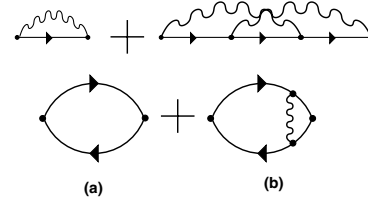


FIG. 1. The NCA [(a)] and the VCA [(a) + (b)] diagrams for electron (upper graphs) and phonon (lower graphs) self-energies. Wavy lines are phonon propagators while straight lines are electron propagators. Second order perturbation theory is obtained replacing internal lines with free propagators.

just like the electron self-energy. Actually, to allow for a safer truncation on the frequency axis, the quantity which is iteratively determined is not the full self-energy, but the difference between this quantity and the result from second order perturbation theory. Zero temperature results are obtained by lowering the temperature until the physically relevant quantities converge [consistently increasing the number of Matsubara frequencies  $N_{\max} = 6/(2T\pi)$ ]. We checked the convergence to  $T = 0$  by monitoring the quasiparticle spectral weight  $Z$  defined as  $Z^{-1} = 1 - [\Sigma(i\omega_{n=1}) - \Sigma(i\omega_{n=0})/2\pi T]$  where  $\omega_n = (2n - 1)\pi T$ . The vanishing of  $Z$  is used within DMFT to characterize the Mott MIT in the repulsive [19] and the pairing transition in the attractive Hubbard models [22]. A vanishing  $Z$  has been found also in the spinful Holstein model [12]. The convergence to  $T = 0$  turns out to depend on both  $\gamma$  (as detailed below, we study  $\gamma = 0.1$  and  $\gamma = 1$  as representative of adiabatic and nonadiabatic regimes, respectively) and  $\lambda$ . Within VCA  $T/t = 3 \times 10^{-3}$  is sufficient to get results representative of the ground state for weak/intermediate coupling. In the spinful case for  $\gamma = 0.1$ ,  $T = 10^{-3}$  is instead necessary since the polaron crossover is approached for smaller coupling (see below). Within NCA it is possible to span the strong-coupling regime, making an extrapolation to  $T = 0$  necessary in the adiabatic regime for  $\lambda > 1$  ( $\lambda > 0.5$ ) in the spinless (spinful) case. In the nonadiabatic regime the extrapolation is required for  $\lambda > 1.6$  ( $\lambda > 1.2$ ) in the spinless (spinful) case.

We first discuss the spinless case. Exact DMFT results for  $Z$  are shown in Fig. 2. The logarithmic scale on the  $y$  axis evidences that in both cases  $Z$ , even if exponentially reduced, never vanishes by increasing  $\lambda$ , indicating that no MIT is taking place. It is important to observe that  $Z$  increases when the truncation error is reduced increasing  $N_s$ . The comparison with NCA and VCA shows non-trivial tendencies. Both approximations are accurate at weak coupling, but VCA remains closer to ED for relatively large coupling even in the adiabatic regime, where the Migdal approximation would be expected to hold. Quite surprisingly even in the nonadiabatic regime VCA improves NCA only at weak coupling. At strong coupling NCA predicts a polaronic crossover, in qualitative agreement with exact results, even if, for  $\gamma = 1$ , the crossover

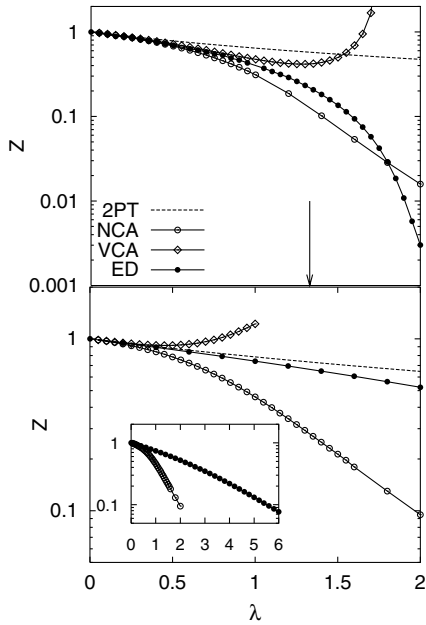


FIG. 2. Spinless fermions. The quasiparticle weight  $Z$  within second order perturbation theory (2PT), NCA, VCA, and ED for  $\gamma = 0.1$  (upper panel) and  $\gamma = 1$  (lower panel) as a function of  $\lambda$ . The arrow in the upper panel marks the MIT for  $\gamma = 0$  [16]. The inset shows ED and NCA in a larger range of  $\lambda$  for  $\gamma = 1$  to make the polaron crossover visible.

coupling is strongly underestimated by NCA. On the other hand, VCA drastically diverges from ED and gives unphysical negative mass renormalization at strong coupling both for  $\gamma = 0.1$  and 1, in agreement with the divergence of vertex corrections predicted in Ref. [11]. The coupling at which the approximate methods deviate from exact results decreases with increasing  $\gamma$ , and it is unrelated to the polaron crossover coupling which is instead larger for  $\gamma = 1$ , as shown in the inset of Fig. 1, and in agreement with the single polaron case [8,9].

An important difference between the finite-density situation and the single polaron problem is that many electrons are able to renormalize the phonon properties. The renormalized phonon frequency can be obtained from the phonon propagator  $D(i\omega_n) = \int_0^\beta d\tau e^{i\omega_n\tau} \langle T[a_0(\tau) + a_0^\dagger(\tau)](a_0 + a_0^\dagger) \rangle$ , as  $(\Omega/\omega_0)^2 = -2/\omega_0 D(i\omega_n = 0)^{-1}$ . As shown in Fig. 3,  $\Omega/\omega_0$  never vanishes as a function of the coupling, but rather exponentially decreases. The way NCA and VCA results for  $\Omega$  compare with ED is analogous to the results for  $Z$ . In the adiabatic regime NCA strongly overestimates  $\Omega/\omega_0$  around the polaron crossover. In the nonadiabatic regime NCA again predicts a phonon softening which does not actually occur at such small values of the coupling. In the same regime VCA improves the NCA result only at weak coupling and gives a phonon hardening at strong coupling. It is worth noting that for both  $Z$  and  $\Omega$  the coupling at which NCA and VCA deviate from ED is lower in the nonadiabatic than in the adiabatic regime. This “nonuniform” behavior is not present for a single

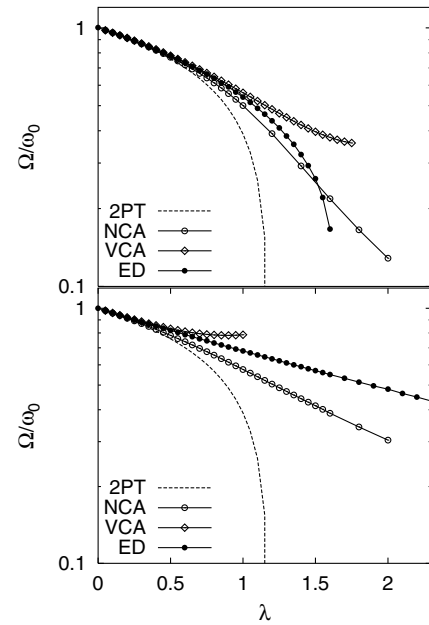


FIG. 3. Spinless fermions. The renormalized phonon frequency  $\Omega/\omega_0$ . Notations are the same as in Fig. 2

polaron [9] and represents a first peculiarity of the finite-density case.

Now we compare our findings for spinless fermions with the spinful fermion case. In the adiabatic regime a MIT has been found around  $\lambda \simeq \lambda_{\text{MIT}} \simeq 0.68$  [17], close to the value ( $\lambda = 0.664$ ) at which the density of state at Fermi energy vanishes in the adiabatic limit ( $\gamma = 0$ ) [16]. This transition has a precursor in the phonon softening [12] but, contrary to the spinless case, the spin degrees of freedom prevent electron coherent hopping at strong coupling through a Kondo-like mechanism [23]. A MIT has been claimed to occur also within NCA [11].

In Fig. 4 we show results for  $\gamma = 0.1$ . The logarithmic plot clearly shows that  $Z$  vanishes faster than the exponential, signaling a MIT at  $\lambda \simeq 0.76$ , in agreement with Ref. [12]. Contrary to the spinless case, here  $Z$  decreases

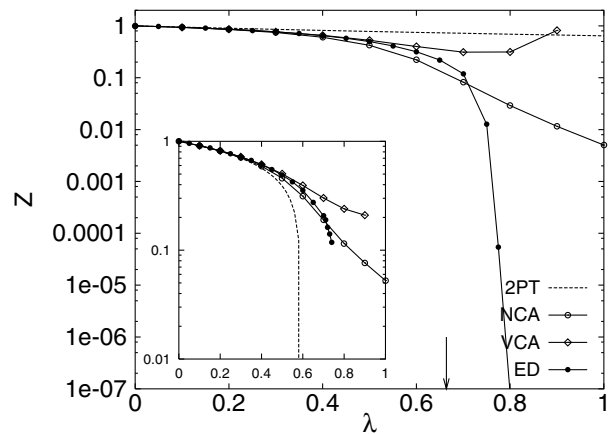


FIG. 4. Spinful fermions.  $Z$  and  $\Omega/\omega_0$  (inset) for  $\gamma = 0.1$  as a function of  $\lambda$ . The arrow marks the MIT for  $\gamma = 0$  [16].

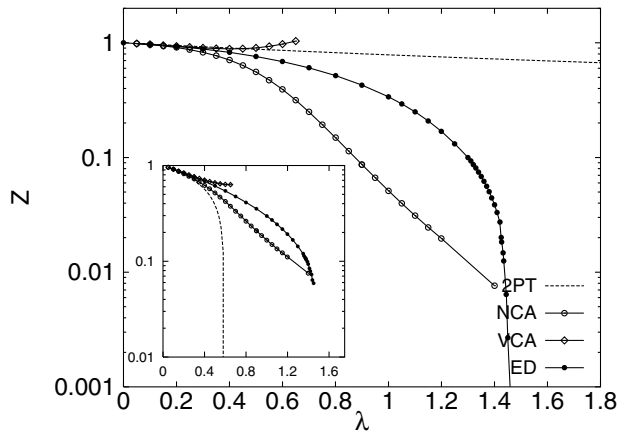


FIG. 5. Spinful fermions.  $Z$  and  $\Omega/\omega_0$  (inset) for  $\gamma = 1.0$  as a function of the coupling.

by increasing  $N_s$ . On the other hand,  $\Omega/\omega_0$  decreases with  $\lambda$  as in the spinless case, suggesting that, even if strongly softened, the phonon mode never becomes completely soft. This behavior is more evident for larger phonon frequency  $\gamma = 1$ , as reported in Fig. 5. Also in this case  $Z$  vanishes much faster than the exponential at  $\lambda = 1.44$ , where the MIT takes place, while the phonon renormalization is much less effective and leads to quite a large value of  $\Omega/\omega_0$  even at the MIT point (see inset).

The comparison with approximate schemes qualitatively resembles the spinless case. NCA underestimates  $Z$  for  $\lambda$  below the MIT, but it gives a finite weight also above the exact MIT point. Our extrapolation to  $T = 0$  from finite temperatures does not allow us to definitively rule out the existence of a MIT within NCA even if, in contrast with a claim in Ref. [11],  $Z$  seems to decrease exponentially with  $\lambda$  within this approximation [24]. Again VCA gives better results than NCA even in the adiabatic regime up to intermediate coupling  $\lambda \approx 0.55$ , but it becomes completely unreliable at strong coupling.

We have studied the formation of a polaronic state in the Holstein model at half filling within DMFT. For spinless fermions, a continuous crossover leads to a polaronic state by increasing the coupling constant. Despite the electron effective mass becoming exponentially large in the strong-coupling regime, the ground state is always metallic. The crossover is more abrupt in the adiabatic case. In the spinful case, the polarons can bind to form bipolarons, leading to a real MIT. The phonon renormalization is much stronger in the adiabatic regime than in the nonadiabatic case, but the phonons do not become completely soft at the MIT. Approximate treatments (NCA and VCA) strongly deviate from exact DMFT above a coupling which diminishes with increasing  $\omega_0/t$ . At weak coupling VCA correctly reproduces the qualitative trends of exact results and improves on NCA.

M. C. thanks the Physics Department of the University of Rome “La Sapienza” and INFM, Unitá Roma 1 for hospitality and financial support. We acknowledge financial support of MIUR Cofin 2001 and enlightening discussions with C. Castellani.

- 
- [1] A. Lanzara *et al.*, *Nature* (London) **412**, 510 (2001).
  - [2] G. Zhao, K. Conder, H. Keller, and K. A. Müller, *Nature* (London) **381**, 676 (1996).
  - [3] O. Gunnarsson, *Rev. Mod. Phys.* **69**, 575 (1997).
  - [4] J. Kortus *et al.*, *Phys. Rev. Lett.* **86**, 4656 (2001).
  - [5] P. Calvani *et al.*, *Phys. Rev. B* **53**, 2756 (1996)
  - [6] M. Riccò *et al.*, *Phys. Rev. B* **67**, 024519 (2003).
  - [7] Here we will be concerned only with small polarons arising from Holstein-like interactions. For the definition of other kinds of polarons see, e.g., J.T. Devreese, *Encyclopedia of Applied Physics* (VCH, Weinheim, 1996).
  - [8] M. Capone, W. Stephan, and M. Grilli, *Phys. Rev. B* **56**, 4484 (1997); S. Ciuchi, F. de Pasquale, S. Fratini, and D. Feinberg, *ibid.* **56**, 4494 (1997).
  - [9] M. Capone, C. Grimaldi, and S. Ciuchi, *Europhys. Lett.* **42**, 523 (1998).
  - [10] A. Alexandrov and J. Ranninger, *Phys. Rev. B* **23**, 1796 (1981).
  - [11] J. P. Hague and N. d’Ambrumenil, *cond-mat/0106355*.
  - [12] D. Meyer, A. C. Hewson, and R. Bulla, *Phys. Rev. Lett.* **89**, 196401 (2002).
  - [13] S. Ciuchi and F. de Pasquale, *Phys. Rev. B* **59**, 5431 (1999).
  - [14] J. K. Freericks, M. Jarrell, and D. J. Scalapino, *Phys. Rev. B* **48**, 6302 (1993); J. K. Freericks, *ibid.* **48**, 3881 (1993).
  - [15] J. K. Freericks, *Phys. Rev. B* **50**, 403 (1994)
  - [16] A. J. Millis, R. Mueller, and B. I. Shraiman, *Phys. Rev. B* **54**, 5389 (1996).
  - [17] P. Benedetti and R. Zeyher, *Phys. Rev. B* **58**, 14320 (1998).
  - [18] A. Dippeler and A. J. Millis, *Phys. Rev. B* **65**, 100301 (2002).
  - [19] A. Georges, G. Kotliar, W. Krauth, and M. J. Rozenberg, *Rev. Mod. Phys.* **68**, 13 (1996).
  - [20] M. Caffarel and W. Krauth, *Phys. Rev. Lett.* **72**, 1545 (1994).
  - [21] We also truncate the phonon Hilbert space introducing a cutoff in the number of phonons  $N_{\text{ph}}$  and always checking for convergence. The truncation is more delicate in the adiabatic regime, where a large number of phonons can be excited. When necessary, we used  $N_{\text{ph}} = 50$ .
  - [22] M. Capone, C. Castellani, and M. Grilli, *Phys. Rev. Lett.* **88**, 126403 (2002).
  - [23] G. Moeller, Q. Si, G. Kotliar, M. Rozenberg, and D. S. Fisher, *Phys. Rev. Lett.* **74**, 2082 (1995).
  - [24] The exponential decay of  $Z$  within NCA shown in Fig. 4 is hardly identified using a linear scale as in Ref. [11].